Temperature-Induced Conformational Change at the Catalytic Site of *Sulfolobus solfataricus* Alcohol Dehydrogenase Highlighted by Asn249Tyr Substitution. A Hydrogen/Deuterium Exchange, Kinetic, and Fluorescence Quenching Study

Francesco Secundo,[‡] Consiglia Russo,[§] Antonietta Giordano,[§] Giacomo Carrea,[‡] Mosè Rossi,[§] and Carlo A. Raia*[,§]

Istituto di Chimica del Riconoscimento Molecolare, Consiglio Nazionale delle Ricerche, Via M. Bianco 9, I-20131 Milano, Italy, and Istituto di Biochimica delle Proteine, Consiglio Nazionale delle Ricerche, Via P. Castellino 111, I-80131 Napoli, Italy

Received March 14, 2005; Revised Manuscript Received June 20, 2005

ABSTRACT: A combination of hydrogen/deuterium exchange, fluorescence quenching, and kinetic studies was used to acquire experimental evidence for the crystallographically hypothesized increase in local flexibility which occurs in thermophilic NAD^+-dependent *Sulfolobus solfataricus* alcohol dehydrogenase (SsADH) upon substitution Asn249Tyr. The substitution, located at the adenine-binding site, proved to decrease the affinity for both coenzyme and substrate, rendering the mutant enzyme 6-fold more active when compared to the wild-type enzyme [Esposito et al. (2003) *FEBS Lett. 539,* 14−18]. The amide H/D exchange data show that the wild-type and mutant enzymes have similar global flexibility at 22 and 60 °C. However, the temperature dependence of the Stern−Volmer constant determined by acrylamide quenching shows that the increase in temperature affects the local flexibility differently, since the K_{SV} increment is significantly higher for the wild-type than for the mutant enzyme over the range 18−45 °C. Interestingly, the corresponding van't Hoff plot (log K_{SV} vs $1/T$) proves nonlinear for the apo and holo wild-type and apo mutant enzymes, with a break at ≈45 °C in all three cases due to a conformational change affecting the tryptophan microenvironment experienced by the quencher molecules. The Arrhenius and van't Hoff plots derived from the k_{cat} and K_M thermodependence measured with cyclohexanol and NAD^+ at different temperatures display an abrupt change of slope at 45−50 °C. This proves more pronounced in the case of the mutant enzyme compared to the wild-type enzyme due to a conformational change in the structure rather than to an overlapping of two or more rate-limiting reaction steps with different temperature dependencies of their rate constants. Three-dimensional analysis indicates that the observed conformational change induced by temperature is associated with the flexible loops directly involved in the substrate and coenzyme binding.

Alcohol dehydrogenase from the archaeon *Sulfolobus solfataricus* (SsADH)[1] is a thermophilic NAD-dependent homotetrameric zinc 150 kDa enzyme whose apo and 2-ethoxyethanol−NAD(H) complex 3D structures have been recently determined (*1*, *2*). The 3D structure of the apo form of the mutant Asn249Tyr, which exhibits increased catalytic activity compared to the wild-type enzyme, has also been solved (*3*). The Asn249Tyr substitution, located at the adenine-binding site, decreases the affinity for both coenzyme and substrate, resulting in a 6-fold increase of the turnover number measured at 65 °C with benzyl alcohol as substrate. Indeed, the rearrangement of loop 248−250 induces an adjustment in the conformation of the neighboring coenzyme binding loop 270−275, which in turn is transmitted to the adjacent loop 46−62 of the substrate domain. The latter segment, which is involved in the substrate binding, is one of the most flexible parts of the wild-type SsADH structure and shows higher thermal factors (*B*-factor) compared to the rest of structure in the mutant enzyme. The *B*-factor vs residue number profile indicates that loop 46−62 has a temperature factor 1.3- and 2.5-fold higher with respect to the average of the main chain of the wild-type and mutant enzyme, respectively (*3*). This apparent increase in local flexibility has been correlated to lack of activation in the mutant enzyme, which is displayed by the wild-type enzyme under mild denaturing conditions. In fact, low concentrations of SDS and GuHCl increase the V_{max} for the wild-type enzyme and leave the mutant V_{max} unaltered (*4*). Although the substitution considerably affects the kinetics of the enzyme, it does not interfere with the structural stability. Indeed, the mutant's resistance to heat, denaturants, and proteases proved similar or even better than the parent protein (*4*).

A combination of hydrogen/deuterium exchange and acrylamide fluorescence quenching studies was used to establish experimentally whether the increase in flexibility is located in specific regions of the mutant enzyme or extended to the whole structure. The peculiarity that the two tryptophan residues present in the SsADH subunit, Trp95

* Corresponding author. Fax: +39-0816132248. E-mail: ca.raia@ibp.cnr.it.

‡ Istituto di Chimica del Riconoscimento Molecolare.

§ Istituto di Biochimica delle Proteine.

[1] Abbreviations: ADH, alcohol dehydrogenase; SsADH, *Sulfolobus solfataricus* ADH; mSsADH, Asn249Tyr mutant of SsADH; apo SsADH, coenzyme-free SsADH; holo SsADH, SsADH−NAD(H) complex.

10.1021/bi050469c CCC: $30.25
Published on Web 07/28/2005

and Trp117, are close to each other within the hydrophobic cluster located in the catalytic site has allowed us to monitor the temperature dependence of fluctuations occurring in the protein matrix surrounding the two fluorophores. Moreover, the hypothesis whether the apparent difference in flexibility between the active sites of the two enzymes could result in different temperature dependence of the kinetic constants was ascertained by Arrhenius and van't Hoff plot analysis, using 1-propanol, cyclohexanol, and NAD^+ as substrates. Both quenching and kinetic studies provide evidence of a temperature-induced conformational change occurring at 45−50 °C at the catalytic site and involving the loops participating in the catalysis of the archaeal alcohol dehydrogenase.

MATERIALS AND METHODS

Chemicals. D_2O and acrylamide were purchased from Fluka (Buchs, Switzerland) and Applichem (Darmstadt, FRG), respectively. NAD^+ and NADH were obtained from Applichem. Cyclohexanol-d_{12} and benzyl-d_7 alcohol were from Aldrich. NADD for FT-IR experiments was prepared by dissolving NADH in a minimum volume of D_2O to remove all exchangeable hydrogens, and the sample was then lyophilized for 24 h and stored protected from water vapor. Other chemicals were A-grade substances from Applichem or Sigma (St. Louis, MO). An 8.0 M acrylamide solution was ultrafiltered through a 0.22 μm filter before being purged with a stream of nitrogen, fractioned in small volumes, and stored frozen at −20 °C. Solutions of NADH and NAD^+ were prepared as previously reported (*5*). All solutions were made up with MilliQ water.

Protein Purification. SsADH and mSsADH were expressed and purified from *Escherichia coli* following a previously described procedure (*4*). Removal of endogenous NAD(H) traces tightly bound to the wild-type SsADH was obtained by exhaustive dialysis as described by Raia et al. (*5*). The holo form of SsADH was obtained by adding a 10-fold normal NADH excess to the apo enzyme.

Determination of Protein Concentration. Protein concentration was determined with a Bio-Rad protein assay kit using bovine serum albumin as standard and introducing a correction factor deduced from quantitative amino acid analysis (*5*).

FT/IR Measurements. The kinetics of H/D exchange in D_2O were measured by Fourier transform infrared spectroscopy on a JASCO FT/IR-610 spectrophotometer. CaF_2 cells with a path length of 100 μm were used for both the sample and background measurements. The temperature was measured by a thermometer inserted directly inside the cell apparatus. Measurements were carried out at 22 ± 0.5 and 60 ± 0.5 °C. The enzyme samples were dialyzed in 4 mM Tris-HCl, pH 7.2, before lyophilization. Aliquots of buffer were also lyophilized and used for background measurements. To initiate the exchange process, 1.3 mg of protonated and dry apo SsADH or mSsADH was dissolved in 120 μL of D_2O. One hundred twenty microliters of D_2O containing 0.45 mg of NADD was used for exchange experiments with holo SsADH. The moment when D_2O was added was taken as the start of the exchange. The enzyme solution in D_2O was centrifuged for 30 s at 12000*g* and then injected into the cell for the measurements. A series of IR spectra (400−4000 cm^{-1} region, resolution of 2 cm^{-1}) were recorded starting 3 min after initiating the H/D exchange. Absorbances of the amide I and amide II bands were measured at 1648 and 1548 cm^{-1}, respectively, and corrected for the baseline absorbance measured at 1750 cm^{-1}. The fraction of the unexchanged peptide hydrogen atoms was determined as

$$X = [\omega(t) - \omega(\infty)]/[\omega(0) - \omega(\infty)]$$

(*6*, *7*) where $\omega(t)$ is the ratio of the amide II and amide I absorbances (A), corrected with the absorbance of the baseline, at time t:

$$\omega(t) = [A_{\text{amideII}}(t) - A_{\text{base}}(t)]/[A_{\text{amideI}}(t) - A_{\text{base}}(t)]$$

$\omega(0)$ is the amide II/amide I ratio of the nondeuterated protein, and $\omega(\infty)$ is the ratio for the fully deuterated protein. A spectrum of the protein in KBr was recorded to measure the $\omega(0)$ value. This proved to be 0.70 and 0.76 for SsADH and mSsADH, respectively. As expected, these values were very similar since the two enzymes differ for only one amino acid residue. The value of $\omega(\infty)$ was obtained from the samples incubated in D_2O at 60 °C for 24 h and resulted in 0.102 ± 0.003 for both of the enzymes. X, the fraction of the unexchanged hydrogens of the peptide, is a function of the time, pH, and temperature. The results were interpreted in terms of the EX_2 mechanism (*7*, *8*), i.e., under the assumption that the protein backbone amide hydrogen bonds actually form and break faster than the rate of exchange of a free amide. In this case, the exchange proceeds as a series of simultaneous first-order reactions:

$$X = n^{-1}\sum_{i=1}^{n}\exp(-\rho_i k_0 t)$$

where n is the number of amide hydrogens per protein molecule and ρ_i is the probability of finding the ith amide exposed to the solvent. k_0 is the exchange rate of an exposed amide proton under the particular conditions of pH and temperature, calculated empirically from the equation:

$$k_0 = (10^{-\text{pHread}} + 10^{\text{pHread}-6}) \times 10^{0.05(T-25)} \times \text{s}^{-1}$$

where T is the temperature in °C. This empirical equation, based on a poly(D,L-alanine) model (*8*), was used in the calculations as a good approximation. However, because the present work is a comparative study of two proteins that differ in only one amino acid residue, the actual value of k_0 does not affect the results. The kinetic data of the exchange were plotted as the ratio of the unexchanged protons, X vs $\log(k_0 t)$, in the form of relaxation spectra. The pH was measured just after the lyophilized proteins were dissolved in D_2O by means of a Jenway pH meter equipped with a Crison glass electrode. The value measured proved constant throughout the H/D exchange kinetics and was used for the k_0 calculation.

Fluorescence Studies. Fluorescence studies were performed with a JASCO FP-777 spectrofluorometer equipped with an external thermocryostated water bath and using a spectrosyl quartz cuvette. Quenching by acrylamide of the intrinsic fluorescence was investigated in the temperature range 18−62 °C by sequentially adding 3 μL aliquots of 8.0 M acrylamide to a 500 μL solution containing the enzyme (0.17 μM tetramer) in 50 mM Tris-HCl, pH 8.8. Emission

was monitored at 328 nm for apo SsADH and at 330 nm for holo SsADH and mSsADH, respectively (λ_{ex} = 297 nm). The pH values of the buffer were controlled at each temperature. Emission intensity values were corrected for dilution and inner filter effect according to Brand and Witholt (*9*). Quenching data were analyzed according to the Stern−Volmer equation:

$$F_0/F = 1 + K_{SV}[Q]$$

where F_0 and F are the emission intensities in the absence and presence of quencher Q, respectively, and K_{SV} is the Stern−Volmer quenching constant (*10*). All measurements were made in triplicate. Although a protein matrix is not a homogeneous fluid, one might still attempt to characterize its structural/dynamic properties in terms of thermodynamic parameters for the inward diffusion of the probe (*11*). The enthalpy of the quenching process was approximated from the slope of the best fit of van't Hoff plots of log K_{SV} versus $1/T$, as $-\Delta H^{\ddagger}/R$, where R is the universal gas constant, 8.314 J K^{-1} mol^{-1}, and T is the absolute temperature. The values $\Delta G^{\ddagger}$ and $\Delta S^{\ddagger}$ characterizing the quenching process were determined using the equations:

$$\Delta G^{\ddagger} = -2.3RT \log K_{SV}$$

$$T\Delta S^{\ddagger} = \Delta H^{\ddagger} - \Delta G^{\ddagger}$$

(*12*). Two charged collisional quenchers, I^-, as KI, and Cs^+, as CsCl, were also used to probe the solvent accessibility and local fluorophore environment (*13*). Potassium iodide stock solutions contained 10^{-4} M sodium thiosulfate to suppress the formation of I_3^-. Studies of the temperature dependence of intrinsic fluorescence were performed by allowing the enzyme samples to stand at the desired temperature for 15 min and by recording the emission spectra following excitation at 280 and 297 nm. The protein concentration used was 0.23 μM for apo SsADH and 0.16 μM for mSsADH, in 50 mM Tris-HCl, pH 8.8. Temperature was controlled in the cuvette and measured in all experiments to within ±0.2 °C. Fluorescence contributions from buffer components were subtracted from all of the spectra. Each spectrum was obtained in duplicate or triplicate with virtually identical results.

Kinetics. The activity was assayed toward cyclohexanol and 1-propanol at a determined temperature as described for the benzyl alcohol standard assay (*5*) using a Cary 1E spectrophotometer equipped with a Peltier effect-controlled temperature cuvette holder. SsADH was assayed in 1 mL of standard assay mixture containing 0.025−1 mM cyclohexanol or 0.125−10 mM 1-propanol, 3 mM NAD^+, and 0.1 M glycine−NaOH buffer (pH 10.5). The mutant enzyme was assayed under the same conditions, this time using 0.025−12 mM cyclohexanol or 0.125−10 mM 1-propanol and 30 mM NAD^+. The kinetic constants for NAD^+ at different temperatures were determined at the fixed concentrations of 2 and 20 mM cyclohexanol for SsADH and mSsADH, respectively, and with varied concentrations of coenzyme. The measurements of kinetic parameters were carried out in duplicate or triplicate, and steady-state kinetic data were analyzed using the program GraFit (*14*). The temperature dependence of the turnover number was analyzed according to the Arrhenius equation (*12*).

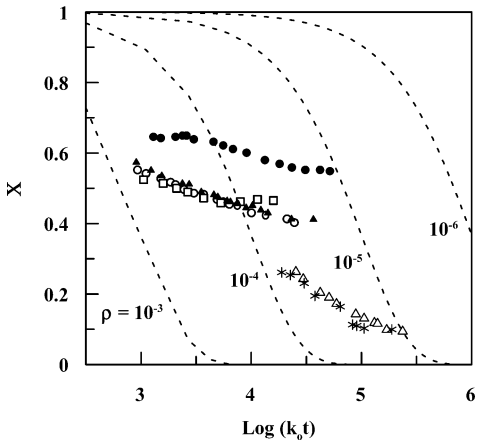

FIGURE 1: H/D exchange data summarized in the form of relaxation spectra for SsADH and mSsADH at 22 and 60 °C: (white circles) apo SsADH, 22 °C, pH 6.9; (white squares) mSsADH, 22 °C, pH 7.1; (white triangles) apo SsADH, 60 °C, pH 6.4; (*) mSsADH, 60 °C, pH 6.3; (black circles) holo SsADH, 22 °C, pH 7.1; (black triangles) holo SsADH, 60 °C, pH 6.6. The enzyme concentration is 71 μM. X is the fraction of unexchanged peptide hydrogens, t is time in seconds, and k_o is the calculated chemical exchange rate constant. The solid lines represent the exchange rate curves for hypothetical polypeptides characterized by the ρ values indicated in the figure. A shift toward smaller ρ values reflects an increase in the conformational rigidity. Overlapping curves reflect similar rigidity.

Studies with Deuterated Alcohols. The catalytic activity of both SsADH and mSsADH on cyclohexanol and benzyl alcohol was measured at 35, 45, 65, and 75 °C with saturating concentrations of alcohol and NAD^+, and the V_{max} values were compared to those obtained with the corresponding deuterated alcohols, cyclohexanol-d_{12} and benzyl-d_7 alcohol, under the same experimental conditions. Each measurement was carried out in triplicate.

Structural Analysis. Structural analysis was done on the basis of the atom coordinates of the apo and holo SsADH (*1*, *2*) and mSsADH (*3*) using the program Swiss-Pdb Viewer v3.7 (*15*). The solvent exposure of residues was evaluated with the program DSSP (*16*). This method, which determines the residue accessibility value to solvent in $Å^2$, establishes whether a residue is exposed or buried if its accessibility is greater or less than 16% compared to the accessibility of a free residue. The crystallographic structure of mSsADH in the holo form has not yet been solved given its very low affinity for coenzyme.

RESULTS

H/D Exchange Study. The global structural flexibility of the wild-type and mutant SsADH was evaluated at 22 and 60 °C, measuring the rate of H/D amide exchange in D_2O by FT/IR spectroscopy. The plots of X vs log(k_0t) are shown in Figure 1.

The exchange curves of the two enzymes in the absence of coenzyme almost coincide both in shape and in position at 22 and 60 °C, reflecting a similar distribution of conformational fluctuations. The relaxation spectra indicate probability distributions. The comparison of the curves of SsADH and mSsADH with those of hypothetical polypeptides exposing their peptide hydrogens in a cooperative way with probability ρ_i indicates that the conformational fluctuations exposing the buried peptide hydrogens to the solvent are

noncooperative for SsADH and mSsADH in the conditions tested. These conformational fluctuations are due to the overlapping of local movements with varying probabilities for various parts of the protein. The shift of the relaxation spectrum toward the right upper corner, i.e., toward smaller ρ values, reflects an increase in the conformational rigidity, which is the case of the two enzymes at 22 °C with respect to 60 °C. De Weck et al. (*17*) found a H/D exchange retardation for yeast ADH upon coenzyme binding with respect to the free enzyme. Interpreting the H/D exchange kinetics data in terms of the EX_2 mechanism, the authors have shown that such retardation is likely due to a pronounced change in the conformational equilibrium between nonexchanging folded conformations and exchanging locally unfolded conformations. The curves recorded at 22 °C and the same pH for the holo and apo forms of SsADH indicate a H/D exchange retardation for the former with respect to the latter (Figure 1). In terms of the EX_2 mechanism, this suggests that, in the case of the archaeal ADH, the exchange retardation observed upon coenzyme binding is likely due to a shift in the conformational equilibrium of the protein toward a nonexchanging folded conformation; i.e., the binary complex formation imposes a somewhat conformational tightening on the enzyme structure. This feature is also evident from the exchanging data at 60 °C, where the holo form of SsADH seems to achieve a structural tightening similar to that of the apo form at 22 °C.

Fluorescence Quenching. The SsADH subunit contains 2 tryptophan residues, Trp95 and Trp117, located within the catalytic domain and 13 tyrosine residues dispersed throughout the structure (*1*). The values of relative accessibility to the solvent of the Trp95 side chain are around 1%, 3.5%, and 1%, while those of the Trp117 side chain are around 7%, 18%, and 10% for the apo and holo SsADH and mSsADH, respectively. This suggests that both residues lie buried in the three structures, although Trp117 is slightly exposed in the holo enzyme structure. Steady-state fluorescence and structural studies recently published (*18*) established the structural basis of dependence of the SsADH intrinsic fluorescence properties on peculiarities of its fluorophore location. Figure 2 shows the Stern−Volmer plot for the acrylamide fluorescence quenching of apo and holo SsADH and mSsADH determined at 18 and 62 °C.

The dependence of quenching on acrylamide concentration is essentially linear, although the holo enzyme shows a slight deviation from linearity at small [Q]. The λ_{max} position (329 nm) for the three proteins reflects the hydrophobic environment surrounding the tryptophan residues (data not shown). This spectral characteristic does not change on quenching. No λ_{max} shift was observed at 18, 34, and 53 °C following the addition of acrylamide up to 0.8 M concentration, indicating that the effect of quenching is nearly equivalent on both residues (data not shown). Furthermore, linearity in the Stern−Volmer plot excludes the occurrence of protein denaturation, since this would have given an upward curving plot. The slope of holo SsADH is lower than that of the apo SsADH, suggesting that an appreciable tightening of the structure around tryptophans and/or a further shielding of these residues from collisions occurs in the presence of coenzyme. It is worth noting that the V_{max} vs [NAD^+] curves for SsADH and mSsADH, determined at 50 °C and using benzyl alcohol as substrate, proved coincident both in the absence and in the presence of 0.4 M acrylamide. This would indicate that the presence of acrylamide at a concentration yielding substantial quenching does not prevent the coenzyme binding or disturb the catalysis mechanism. Figure 3 shows the effect of temperature on the Stern−Volmer constant as determined in the range 18−62 °C for the apo and holo SsADH and mSsADH.

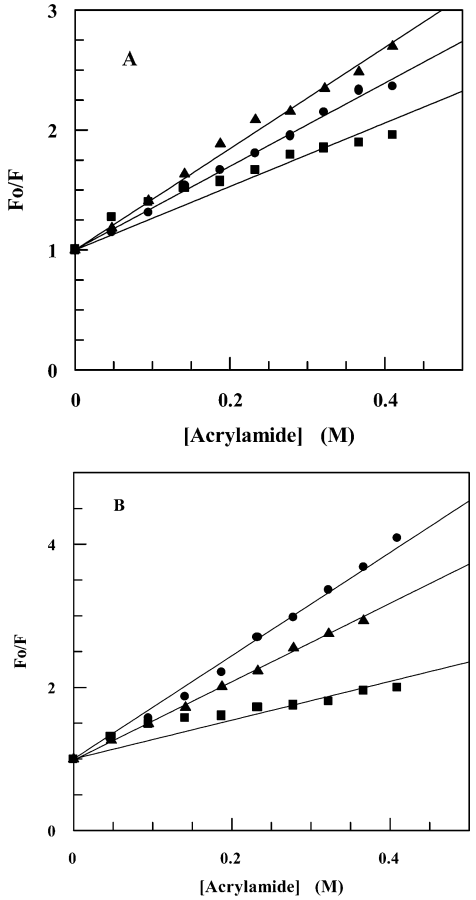

FIGURE 2: Representative Stern−Volmer plot for the acrylamide quenching of apo (circles) and holo (squares) SsADH and mSsADH (triangles) determined at 18 (panel A) and 62 °C (panel B). The buffer was 50 mM Tris-HCl, pH 8.8. Excitation and emission wavelengths = 297 and 329 nm, respectively.

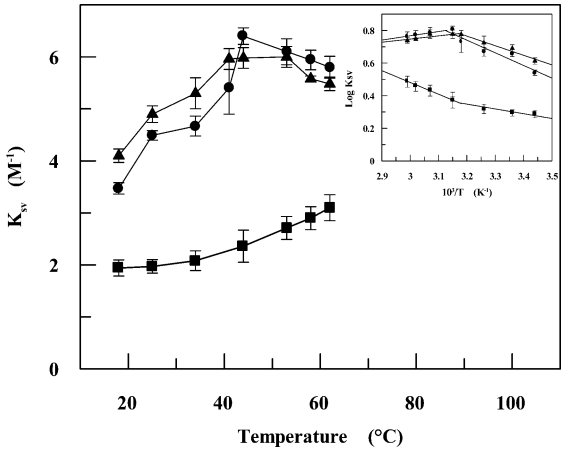

FIGURE 3: Acrylamide quenching of apo (circles) and holo SsADH (squares) and mSsADH (triangles) as a function of temperature. The values of K_{SV} were determined at each temperature as described in Figure 2 and represent the average of three measurements. The inset shows the van't Hoff plot of the same data. Error bars represent the SD from three independent experiments.

Table 1: Thermodynamic Parameters for Acrylamide Quenching of Apo and Holo SsADH and Apo mSsADH[a]

enzyme	$\Delta G^{\ddagger}$ (kJ mol^{-1})		$\Delta H^{\ddagger}$ (kJ mol^{-1})		$T\Delta S^{\ddagger}$ (kJ mol^{-1})	
apo SsADH	−3.9	−4.9	12.2	−7.7	16.1	2.8
mut SsADH	−4.2	−4.7	8.7	−6.5	12.9	11.2
holo SsADH	−2.2	−2.9	3.1	10.8	5.3	13.7

[a] The $\Delta H^{\ddagger}$ values are from the inset of Figure 3 and refer to the lower (left column) and higher (right column) temperature segment of the van't Hoff plots. $\Delta G^{\ddagger}$ and $T\Delta S^{\ddagger}$ were calculated according to the relationship reported in Materials and Methods and refer to 34 (left column) and 58 °C (right column). SD = ±10%.

Table 2: Primary Deuterium Kinetic Isotope Effects on SsADH and mSsADH at Different Temperatures

	$V_{H/D}$[a] (SsADH)		$V_{H/D}$ (mSsADH)	
T (°C)	CE	BzOH	CE	BzOH
35	1.2	1.1	2.0	1.2
45	1.3	1.1	2.3	1.1
65	1.2	1.1	2.5	1.5
75	1.4	1.2	2.4	1.4

[a] $V_{H/D}$ represents the ratio between the V_{max} values for nondeuterated and deuterated alcohol oxidation, measured at the indicated temperatures at saturating concentrations of both alcohol and coenzyme. CE = cyclohexanol;, BzOH = benzyl alcohol. SD = ±10%.

The K_{SV} values at 18 °C for apo SsADH and mSsADH are 3.5 and 4.1 M^{-1}, respectively, before increasing to about 45 °C and slightly decreasing at higher temperatures. More importantly, the K_{SV} increment is higher for apo SsADH (by 1.9 times) than mSsADH (1.2 times) in the range 18−45 °C. However, the K_{SV} for the SsADH holo form is significantly lower and increases less sharply along the entire temperature range (its value is 2.0 and 3.1 M^{-1} at 18 and 64 °C, respectively). The addition of KI and CsCl, two charged and hydrated quenchers, up to a 0.4 M concentration, only yielded a negligible drop in fluorescence intensity for all three ADHs, thus indicating that the environment crossed by the inwardly penetrating neutral acrylamide molecules is mainly hydrophobic (data not shown). Overall, these results suggest that the accessibility of acrylamide to fluorophores is higher in the mutant than in the wild-type enzyme, although it is less temperature-dependent in the former due to the intrinsic loosening of its structural segments experienced by acrylamide. The slight decrease in K_{SV} occurring between 50 and 60 °C for the two apo forms (Figure 3) is worth noting. An increase in hydrophobic interactions with temperature at least up to 60 °C has been reported to occur in proteins (*19*), and the hydrophobic effect is a common strategy of thermophilic enzymes to delay the point of denaturation and maintain a certain functional state. The hydrophobic effect that occurs throughout the SsADH structure is revealed by acrylamide quenching as a subtle structural tightening of the region surrounding the two fluorophores. The temperature dependence of the Stern−Volmer constant fitted to the van't Hoff equation (Figure 3, inset) shows a convex plot for apo SsADH and mSsADH, and a concave plot for the holo SsADH, with a transition temperature around 45 °C in all three cases. Presumably, the cause of this discontinuity is a conformational change occurring in the sphere of action of acrylamide. This conformational change occurs in all three structures but displays a different K_{SV} temperature dependence for the apo and holo forms of the wild-type enzyme. Table 1 gives the thermodynamic parameters characterizing the quenching process for the three enzyme forms calculated at two representative temperatures of the biphasic curves, 34 and 58 °C.

The energy barrier to the quenching process for apo SsADH and mSsADH is similar and comprises unfavorable ΔH and favorable ΔS terms below the transition temperature. Above the transition temperature the quenching process is enthalpically favored and entropically unfavored. This suggests that the conformational change is characterized by small structural rearrangements involving van der Waals, hydrogen bonds and a reordering of infrastructural water molecules. The $\Delta G^{\ddagger}$ value for holo SsADH is relatively higher at low temperature, reflecting a more difficult quenching process (relatively lower values of K_{SV}) characterized by a large decrease in both the enthalpic and entropic terms when compared to apo SsADH values. The quenching process is rendered easier above the transition temperature by $\Delta\Delta G^{\ddagger}$ = 0.7 kJ/mol. However, unlike the apo form, both the entropic and enthalpic terms for the holo form increase on transition, and the increase in the former implies a structural disorder increase. This increase reflects the cleavage or weakening of H bonds and/or hydrophobic interactions.

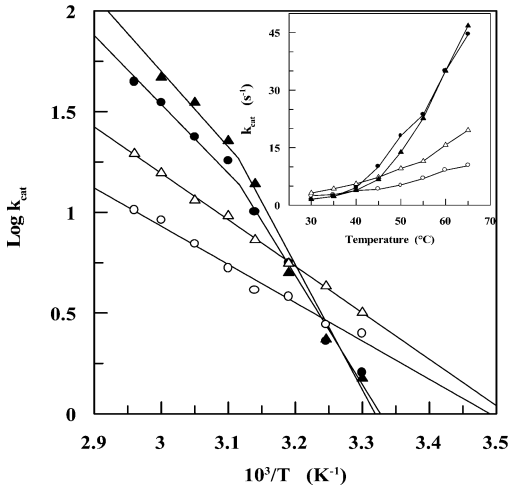

FIGURE 4: Arrhenius plots from the thermophilicity curves determined for SsADH (white symbols) and mSsADH (black symbols). Substrate: cyclohexanol (circles) and 1-propanol (triangles). The inset shows the dependence of k_{cat} on temperature yielding data of the main plot. Each V vs [alcohol] curve was obtained at the determined temperature as described in Materials and Methods, using saturating NAD$^+$ concentrations.

Deuterium Kinetic Isotope Effect. Table 2 lists the kinetic isotope effects on $V_{max}{}^{H}/V_{max}{}^{D}$ determined on SsADH and mSsADH.

The wild-type enzyme does not display any isotope effect with cycloexhanol and benzyl alcohol, whereas the mutant enzyme shows a slight isotope effect only with the former substrate. These data suggest that, over the temperature range 35−75 °C, the limiting step of the overall reaction rate for SsADH is the last step, namely, the NADH dissociation, while for the mutant enzyme it is partially the third step, i.e., the interconversion of the ternary complex (*4*).

Temperature Effect on Kinetic Parameters. The effect of temperature on catalytic turnover and substrate affinity of the two ADHs has been analyzed using 1-propanol and cyclohexanol as substrates in the range 30−65 °C. Figure 4 shows the Arrhenius plots derived from the k_{cat} thermo-

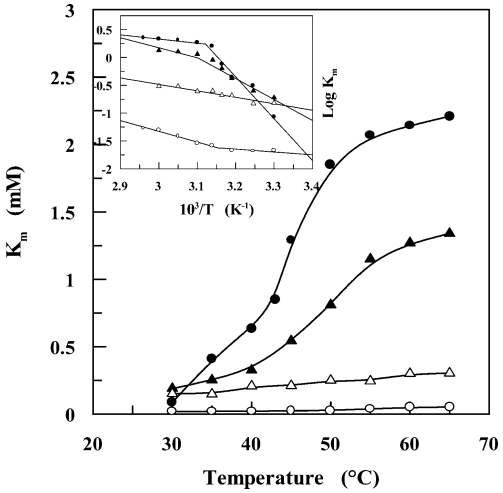

FIGURE 5: Dependence of SsADH (white symbols) and mSsADH (black symbols) substrate affinity on temperature. K_m values for cyclohexanol (circles) and 1-propanol (triangles) were determined by kinetic data used for Figure 4. The inset shows the van't Hoff plot of the same data.

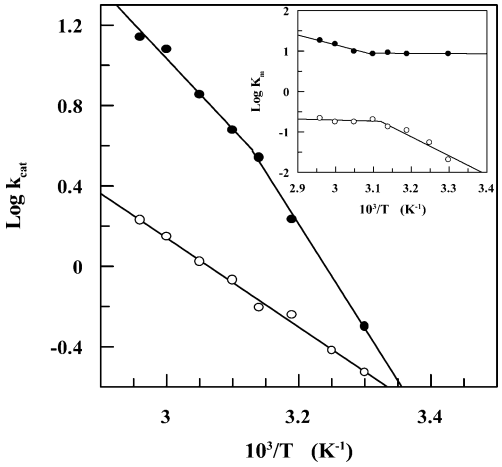

FIGURE 6: Effect of temperature on the reduction reaction of NAD^+ and on the coenzyme affinity for SsADH (white symbols) and mSsADH (black symbols). Arrhenius (main graph) and van't Hoff (inset) plots are from V vs [S] curves, determined at a fixed saturating cyclohexanol concentration and varied coenzyme concentrations as described in Materials and Methods.

dependence curves of the two enzymes determined with the two substrates.

The mutant enzyme displays a discontinuity for the reaction with cyclohexanol and 1-propanol at about 50 °C, while the wild-type enzyme displays linearity with both alcohols. This result agrees with that obtained with benzyl alcohol for which the Arrhenius plot proved linear with the wild-type enzyme and convex for the mutant enzyme with the break centered at 50 °C (*4*). Since the Arrhenius plot essentially represents the temperature effect on the overall reaction rate, it is reasonable to infer that the discontinuity is due to a conformational change in the protein affecting differently the rate constants which characterize the rate-limiting step below and above the transition temperature.

Temperature has markedly different effects on the K_M of SsADH and mSsADH (Figure 5).

The K_M of the mutant enzyme for the two alcohols increases abruptly as the temperature increases, whereas the K_M of the wild-type enzyme increases gradually. It is worth noting that the difference in affinity of the wild-type enzyme for the two alcohols remains constant throughout the entire temperature range, whereas the affinity of the mutant enzyme is similar between 30 and 35 °C, before diverging progressively as the temperature increases. The K_M vs $1/T$ plots (Figure 5, inset) reveal more pronounced differences than those shown by the Arrhenius plots. At around 50 °C, mSsADH exhibits a clearer break with cyclohexanol compared to 1-propanol. The wild-type enzyme displays similar though less accentuated behavior, since the plot is linear with 1-propanol and slightly bent with cyclohexanol.

Figure 6 shows the effect of temperature on k_{cat} and K_M of SsADH and mSsADH determined in the range 30−65 °C, using NAD^+ as substrate and a fixed cyclohexanol concentration.

The Arrhenius plot is linear for SsADH and slightly bent for mSsADH, while the K_M vs $1/T$ plot shows a downward and upward discontinuity with the former and latter, respectively, with the bend at 48−50 °C. K_M is a complex function of the rate constants of several of the intermediate steps in the reaction catalyzed by ADH. This involves substrate association, product dissociation, and ternary complex interconversion (e.g., ref *20*), so that the change in slope at the transition temperature seems to reflect the resulting effect of temperature on these steps rather than merely representing the sole effect on the substrate binding affinity.

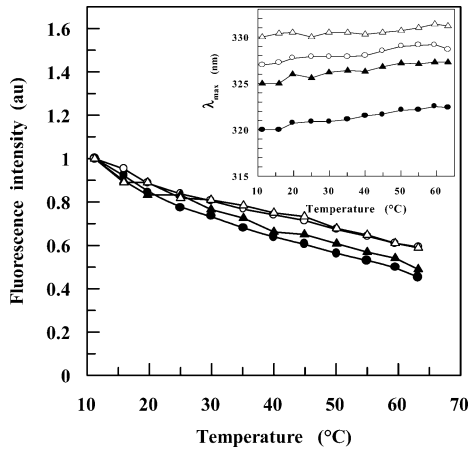

FIGURE 7: Effect of temperature on steady-state fluorescence emission of apo SsADH (circles) and mSsADH (triangles) excited at 280 (black symbols) and 297 nm (white symbols). For each curve, the values of emission intensity are presented as normalized to the value obtained at 11 °C. The inset describes the temperature dependence of the emission fluorescence spectral position (λ_{max}) of the two proteins excited at 280 and 297 nm (same symbols as in the main plot). The excitation and emission slit bandwidths were 10 and 5 nm, respectively, and the data interval was 0.1 nm. The protein concentration was 0.23 μM (SsADH) and 0.16 μM (mSsADH), in 50 mM Tris-HCl, pH 8.8. pH values of the buffer were controlled at each temperature.

Temperature Effect on Tertiary Structure. The effect of temperature on the wild-type and mutant enzyme fluorescence has been investigated up to an instrumental limit of 65−70 °C. The intensity of fluorescence emission from each of the two proteins gradually decreases following excitation at 280 and 297 nm as the temperature rises from 10 to 65 °C (Figure 7), with no change around the transition temperature observed by acrylamide quenching and kinetic investigations.

Table 3: Substrate Contacts in Holo SsADH

2-ethoxyethanol interacting atoms O1−C1−C2−O2−C3−C4	interacting residues
O1	**Ser40**[a]
C1	Val296, Trp95
C2	Leu272, Ile120, Phe49
O2	*Leu272*, *Leu295*
C3	Phe49, Leu272, LeuB286[b]
C4	Phe49, Trp117, Ile120, LeuB286[b]

[a] The H-bond contact is shown in bold, whereas the hydrophobic contacts between C atoms within 4.5 Å distance are listed in lightface type. Destabilizing contacts between O and C atoms are shown in italics. [b] With the exception for this residue, all of the other residues belong to the A subunit (from ref *2*).

The profiles at $\lambda_{ex} = 280$ nm parallel those at 297 nm, thus agreeing with the early observation that the SsADH fluorescence emission is dominated by tryptophan fluorescence following excitation at 280 nm (*18*). Figure 7 (inset) shows that the position of the emission maximum shifts with increasing temperature by 1.5 ± 0.5 nm toward a longer wavelength for apo SsADH and mSsADH. The slight red shift suggests a very small increase in polarity in the microenvironment surrounding the two indole rings. This also indicates that a gradual thermal expansion of the whole molecule over the temperature range allows only a very limited access of the solvent to the tryptophan residues.

Structure Analysis. The SsADH 3D tetramer is a dimer of dimers, denoted as AB and CD (*1*). The monomer (37.5 kDa) is formed by the coenzyme-binding domain and the catalytic domain, separated by a cleft containing a deep pocket accommodating both the substrate and the NAD moiety of the coenzyme (*2*). The SsADH subunit undergoes a substantial conformational change on coenzyme binding, characterized by a large rotation (11°) of the catalytic domain relative to the coenzyme domain and by a structural rearrangement of loop 46−62 and loop 270−275 at the domain interface (*2*). These two loops and a third segment, loop 248−250, mutually interact and play an important role in the catalytic function of SsADH, as they are directly involved in the coenzyme and substrate binding. Loop 46−62, in the apo form, extends to cover the active site but changes its conformation upon coenzyme binding to allow the substrate to accommodate in the hydrophobic pocket (Figure 8A). In doing so, residues 46−62 move as a rigid body within the catalytic domain, moving away from the active site and toward loop 270−275 on the coenzyme binding domain.

Loop 46−62 shows higher thermal factors (*B*-factor) compared to the rest of structure, and these factors increase upon the Asn249Tyr substitution (*3*). Asn248 binds to the adenine ring of the coenzyme through an amino−aromatic interaction while Asn249 interacts with Gly271 of the adjacent loop 270−275. The latter displays several interactions with the coenzyme molecule and also interacts with the third loop 46−62 through the contacts Gly274−Gly50 and Leu272−Phe49 (ref *2*, Figure 8A). Table 3 lists the interactions which held the 2-ethoxyethanol molecule in its site as seen from an analysis of the holo SsADH structure (*2*).

The location of the two tryptophan residues is quite peculiar. Within the monomer the two residues are quite close to each other, i.e., 5.8 and 5.6 Å in the apo and holo forms, respectively. However, the distance between Trp95 and Trp117 of monomer A and their counterparts in monomers B, C, and D ranges from 30 to 50 Å. In the apo structure, they form a hydrophobic cluster together with Pro94, Pro115, and Phe49 and also belong to the hydrophobic substrate binding pocket together with I120, L272, L295, and V296 as well as F49 and L58 of loop 46−62 in the holo structure (Figure 8B). Presumably, the presence of the two proline residues, Pro94 and Pro115, contributes to the stiffness of the hydrophobic cluster. It is also worth noting that Leu272 and Val296 interact with the substrate, as well as with the ribose and amide group of the nicotinamide.

DISCUSSION

The results of the amide H/D exchange experiments show that the wild-type SsADH and its Asn249Tyr mutant have similar global flexibility at two very different temperatures; i.e., the overall conformational flexibility of SsADH is not affected by a single-point mutation. Although an increment of approximately 40 °C increases the global flexibility of the two proteins to the same extent, it affects local flexibility differently, as shown by the fluorescence quenching results. The fluorescence studies support the early crystallographic evidence (*3*) that the Asn249Tyr substitution induces an increase in flexibility only in the region involved in the catalysis. However, the greater change in local flexibility with temperature for SsADH with respect to that of mSsADH cannot account for the greater increase in turnover which occurs for mSsADH with respect to SsADH along the same temperature range. The activation mechanism previously proposed is thus confirmed (*4*), i.e., that the increased catalytic activity of the mutant enzyme is due to the faster release of the coenzyme as a direct consequence of the major weakening of the binary complex.

It is hypothesized that the wild-type enzyme exists in two conformational states above and below the break point. Following conformational change, the thermophilic enzyme seems to shift from a quiescent state to one with proper catalytic competence characterized by increasing turnover and decreasing affinities for substrate and coenzyme with temperature. It is worth noting that the K_{SV} vs T profile of holo SsADH roughly parallels the thermophilicity profile, thus underlining the importance of local flexibility for both enzyme catalysis and substrate binding. Although this concept was first reported nearly 5 decades ago (*21*), it has been shown in recent years that the local increase in flexibility is an adaptive strategy of psychrophilic enzymes (*22*) and that it is linked to the efficiency of enzymatic hydride transfer (*23*).

A considerable body of literature exists reporting that thermophilic enzymes are activated by a loosening of their rigid structure in the presence of protein perturbants (*24*, *25*). The present study supports the previous conclusion that dilute denaturants activate SsADH by inducing an increased flexibility at the active site, whereas the mutant enzyme is less sensitive to this effect due to intrinsic loosening of the active site structure (*3*).

The temperature-induced conformational change revealed by fluorescence and kinetic studies and highlighted by the Asn249Tyr substitution is related to specific structural

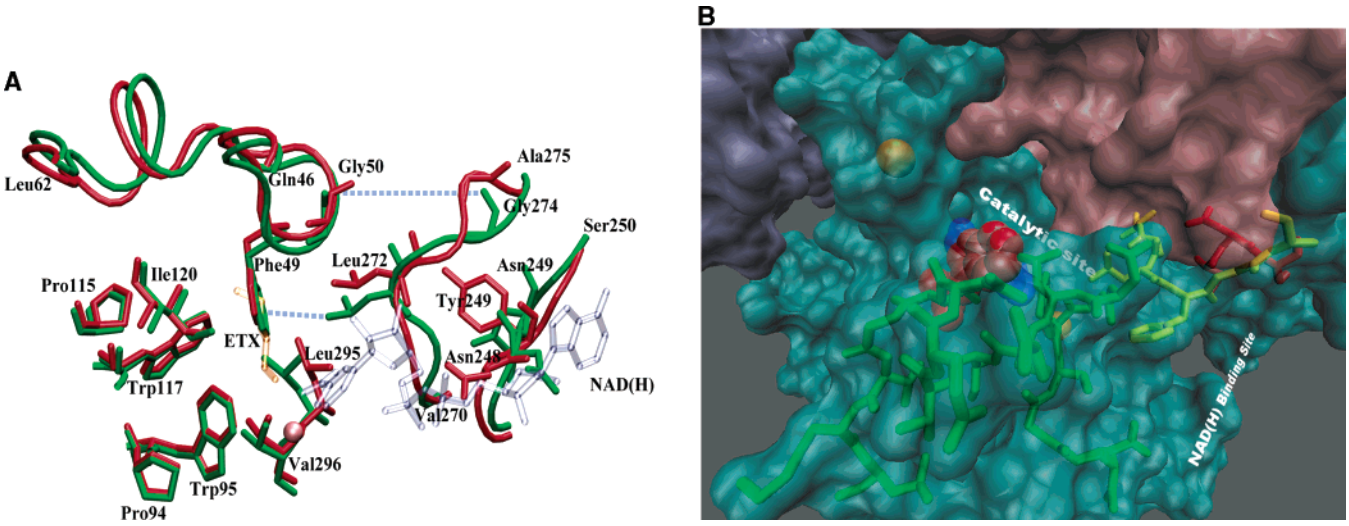

FIGURE 8: (A) Effect of the substitution Asn249 → Tyr in the active site of SsADH and peculiarities of the microenvironment of the Trp residues. The backbones of loops 248−250, 270−275, and 46−62 of apo SsADH (green) and mSsADH (red) are shown superimposed together with the NAD(H) (gray) and substrate ETX molecule (orange) from the holo SsADH structure. Dotted lines indicate the interactions Phe49−Leu272 and Gly50−Gly274 which lock the two loops, 270−275 and 46−62, in the SsADH structure and are lost in the mutant structure. The residues' side chains in the apo SsADH and mSsADH structures are shown in green and red, respectively. Trp95 and Trp117 form a hydrophobic cluster together with Phe49, Pro94, and Pro115 and participate in the substrate binding together with Phe49, Ile120, Leu272, Leu295, and Val296 residues. In the holo SsADH structure, Val270, Leu272, and Val296 residues form H-bond interactions (not shown) with the ribose and nicotinamide moieties, and the Asn248 residue interacts with the adenine ring. The pink sphere represents the catalytic zinc atom. For the sake of clarity, the other residues forming the Trp residue microenvironment (*18*) are not shown. This picture was prepared using VMD (*25*) and POV-Ray (copyright 2003−2004, Persistence of Vision Raytracer Pty. Ltd.). (B) Surface representation of the location of Trp95 (blue) and Trp117 (red) in the apo structure of SsADH viewed from the entrance of the active site of subunit A (cyan). Portions of subunits B and C are visible in pink and purple, respectively. Loops 46−62, 248−250, and 270−275 in stick representation are colored in green, yellow, and red, respectively. The large and middle yellow sphere represents the structural and catalytic zinc atom, respectively. The coenzyme binding site and the substrate binding pocket are indicated. This picture was prepared using VMD (*26*). The structures of apo and holo SsADH and Asn249Tyr SsADH were taken from the 1JVB (*1*), 1R37 (*2*), and 1NTO (*3*) crystal structures, respectively.

elements directly involved in the SsADH catalysis. Moreover, the fact that this conformational change occurs in the absence as well as in the presence of coenzyme suggests that it is not related to the large rotation of the catalytic domain relative to the coenzyme domain. This feature presents an interesting analogy with the recent observation (*23*) that the two cooperative structural changes detected at 35 and 45 °C in *Bacillus stearothermophilus* ADH (htADH) by H/D exchange and mass spectrometry studies are restricted to a small subset of peptides that surround the substrate-binding pocket and are not related to domain opening/closing. Both SsADH and htADH are homotetrameric, and their structures appear almost superimposable (*27*). Loops 46−62 and 270−275 participating in the catalysis of SsADH are found to correspond to segments 46−63 and 260−265 included in peptides **3** and **17**, respectively, of the htADH sequence (*23*, *27*). Peptide **3** resides in the substrate-binding domain and shows a transition in H/D exchange at around 30 °C, while peptide **17**, which is in direct contact with the coenzyme, shows a transition above 40 °C (*23*). Interestingly, although the optimal temperatures of the archaeal and bacterial ADH differ by about 25 °C, the two enzymes seem to attain full active conformation within the same temperature range of 40−50 °C.

The van't Hoff plots show that the change in slope at the transition temperature is more abrupt with large rather than small substrates. It is reasonable to assume that the interactions of the 1-propanol chain O1−C1−C2−C3 with the SsADH binding pocket are similar to those displayed by the 2-ethoxyethanol chain segment O1−C1−C2−O3. Presumably, the interactions displayed by 1-propanol are not sufficiently extended to sense the conformational change induced by temperature, and this results in the linearity of the van't Hoff plot observed for SsADH with this substrate (Figure 5). However, the conformational change that occurs is made more visible by the cyclohexanol and NAD^+ molecules via a different temperature dependence of K_M below and above the transition temperature. This difference is considerable for the bulkier coenzyme molecule because of the higher number of interactions with several residues of the coenzyme-binding and catalytic domain (*2*). The conformational change should involve not only the residues of loop 270−275 but also the nearby segment 248−250, since the residue Asn248 side chain interacts directly with the adenine ring. Detailed knowledge of the substrate and coenzyme interactions with the respective binding pockets of the mutant enzyme would require the availability of the holo mSsADH structure; should this not prove possible, it could be provided by docking studies.

The discontinuity in the Arrhenius and van't Hoff plots at nearly the same temperature (45−50 °C) as illustrated by kinetic and fluorescence quenching studies is proof of the same conformational change. One highly peculiar structural feature of the SsADH molecule is that the indole rings of both tryptophan residues, which are targets of acrylamide, belong to the hydrophobic core constituted by amino acid residues of loops 46−62 and 270−275, both of which are involved in the rearrangement induced by the mutation. Quenchers decrease the fluorescence intensity of the tryptophan residues via physical contact with the excited indole ring; hence the ease of quenching depends on the exposure of fluorophore to the quencher. Quenching is therefore

sensitive to motions that allow quencher molecules to penetrate into the core of proteins and interact with buried tryptophan residues (*10*). The local fluctuations in the protein matrix which allow the inward diffusion of a quencher molecule are very subtle, and their frequency depends on thermal energy; they will also be larger for the protein segments endowed with higher intrinsic flexibility (*11*). The conformational change induced by temperature in SsADH is therefore sensed as the dependence of the Stern−Volmer constant on the effect that temperature exerts on the microenvironment surrounding the two tryptophan residues and experienced by acrylamide.

This study provides evidence that a temperature-induced conformational change occurs at the catalytic site of the thermophilic alcohol dehydrogenase involving the loops participating in catalysis that are endowed with high flexibility. Asn249Tyr substitution not only has highlighted but has actually revealed this conformational change. The fact that the two Trp residues are very close to each other and tightly packed in a hydrophobic cluster situated a short distance from the substrate and coenzyme moieties and embedded within the area of the three flexible loops involved in the catalysis provides us with a useful tool for further studies on function and conformational dynamics.

ACKNOWLEDGMENT

We thank Dr. F. Febbraio for insight and helpful discussion.

REFERENCES

1. Esposito, L., Sica, F., Raia, C. A., Giordano, A., Rossi, M., Mazzarella, L., and Zagari, A. (2002) Crystal structure of the alcohol dehydrogenase from the hyperthermophilic archaeon *Sulfolobus solfataricus* at 1.85 Å resolution, *J. Mol. Biol. 318*, 463−477.
2. Esposito, L., Bruno, I., Sica, F., Raia, C. A., Giordano, A., Rossi, M., Mazzarella, L., and Zagari, A. (2003) Crystal structure of a ternary complex of the alcohol dehydrogenase from *Sulfolobus solfataricus*, *Biochemistry 42*, 14397−14407.
3. Esposito, L., Bruno, I., Sica, F., Raia, C. A., Giordano, A., Rossi, M., Mazzarella, L., and Zagari, A. (2003) Structural study of a single-point mutant of *Sulfolobus solfataricus* alcohol dehydrogenase with enhanced activity, *FEBS Lett. 539*, 14−18.
4. Giordano, A., Cannio, R., La Cara, F., Bartolucci, S., Rossi, M., and Raia, C. A. (1999) Asn249Tyr substitution at the coenzyme binding domain activates *Sulfolobus solfataricus* alcohol dehydrogenase and increases its thermal stability, *Biochemistry 38*, 3043−3054.
5. Raia, C. A., Giordano, A., and Rossi, M. (2001) Alcohol dehydrogenase from *Sulfolobus solfataricus*, *Methods Enzymol. 331* (Part B), 176−195.
6. Závodszky, P., Kardos, J., Svingor, Á., and Petsko, G. A. (1998) Adjustment of conformational flexibility is a key event in the thermal adaptation of proteins, *Proc. Natl. Acad. Sci. U.S.A. 95*, 7406−7411.
7. Kohen, A., and Klinman, J. P. (2000) Protein flexibility correlates with degree of hydrogen tunneling in thermophilic and mesophilic alcohol dehydrogenase, *J. Am. Chem. Soc. 122*, 10738−10739.
8. Hvidt, A., and Nielsen, S. O. (1966) Hydrogen exchange in proteins, *Adv. Protein Chem. 21*, 287−386.
9. Brand, L., and Witholt, B. (1967) Fluorescence measurements, *Methods Enzymol. 11*, 776−856.
10. Eftink, M. R., and Ghiron, C. A. (1976) Exposure of tryptophanyl residues in proteins. Quantitative determination by fluorescence quenching studies, *Biochemistry 15*, 672−680.
11. Eftink, M. R., and Ghiron, C. A. (1977) Exposure of tryptophanyl residues and protein dynamics, *Biochemistry 16*, 5546−5551.
12. Segel, I. S. (1975) Effect of pH and temperature, in *Enzyme Kinetics*, pp 926−941, John Wiley and Sons, New York.
13. Lakowicz, J. R. (1999) *Principles of Fluorescence Spectroscopy*, pp 237−266, Kluver Academic/Plenum Publishers, New York.
14. Leatherbarrow, R. J. (1992) GraFit Version 3.09b, Erithacus Software Ltd., Staines, U.K.
15. Guex, N., and Peitsch, M. C. (1997) SWISS-MODEL and the Swiss-PdbViewer: An environment for comparative modeling, *Electrophoresis 18*, 2714−2723.
16. Kabsch, W., and Sander, C. (1983) Dictionary of protein secondary structure: pattern recognition of hydrogen-bonded and geometrical features, *Biopolymers 22*, 2577−2673.
17. De Weck, Z., Pande, J., and Kagi, J. H. R. (1987) Interdependence of coenzyme-induced conformational work and binding potential in yeast alcohol and porcine heart lactate dehydrogenases: a hydrogen−deuterium exchange study, *Biochemistry 26*, 4769−4776.
18. Giordano, A., Russo, C., Raia, C. A., Kuznetsova, I. M., Stepanenko, O. V., and Turoverov, K. K. (2004) Highly absorbing in UV region complex in selenomethionine-substituted alcohol dehydrogenase from *Sulfolobus solfataricus*, *J. Proteome Res. 3*, 613−620.
19. Scheraga, H. A., Nemethy, G., and Steinberg, I. Z. (1962) The contribution of hydrophobic bonds to the thermal stability of protein conformations, *J. Biol. Chem. 237*, 2506−2508.
20. Plapp, B. V. (1973) On calculation of rate and dissociation constants from kinetic constants for the ordered Bi Bi mechanism of liver alcohol dehydrogenase, *Arch. Biochem. Biophys. 156*, 112−114.
21. Linderstrøm-Lang, K. U., and Schellman, J. A. (1959) Protein structure and enzyme activity, in *The Enzymes* (Boyer, P., Ed.) pp 443−510, Academic Press, New York.
22. Feller, G. (2003) Molecular adaptations to cold in psychrophilic enzymes, *Cell. Mol. Life Sci. 60*, 648−662.
23. Liang, Z. X., Lee, T., Resing, K. A., Ahn, N. G., and Klinman, J. P. (2004) Thermal-activated protein mobility and its correlation with catalysis in thermophilic alcohol dehydrogenase, *Proc. Natl. Acad. Sci. U.S.A. 101*, 9556−9561.
24. Fontana, A., De Filippis, V., Polverino de Laureto, P., Scaramella, E., and Zambonin, M. (1998) Rigidity of thermophilic enzymes, in *Stability and Stabilization in Biocatalysis* (Ballestreros, A., Plou, F. J., Iborra, J. L., and Halling, P. J., Eds.) Vol. 15, pp 277−294, Elsevier Sciences, Amsterdam.
25. Žoldák, G., Šut'ák, R., Antalík, M., Sprinzl, M., and Sedlák, E. (2003) Role of conformational flexibility for enzymatic activity in NADH oxidase from *Thermus thermophilus*, *Eur. J. Biochem. 270*, 4887−4897.
26. Humphrey, W., Dalke, A., and Schulten K. (1996) VMD: visual molecular dynamics, *J. Mol. Graphics 14*, 33−38.
27. Ceccarelli, C., Liang, Z. X., Strickler, M., Prehna, G., Goldstein, B. M., Klinman, J. P., and Bahnson, B. J. (2004) Crystal structure and amide H/D exchange of binary complexes of alcohol dehydrogenase from *Bacillus stearothermophilus*: insight into thermostability and cofactor binding, *Biochemistry 43*, 5266−5277.

BI050469C